Acta Neuropathologica (2019) 138:49–65
https://doi.org/10.1007/s00401-019-01999-w

ORIGINAL PAPER

ADAR2 mislocalization and widespread RNA editing aberrations in C9orf72-mediated ALS/FTD

Stephen Moore[1,2] · Eric Alsop[3] · Ileana Lorenzini[1] · Alexander Starr[1] · Benjamin E. Rabichow[1] · Emily Mendez[1] · Jennifer L. Levy[1] · Camelia Burciu[1] · Rebecca Reiman[3] · Jeannie Chew[4] · Veronique V. Belzil[4] · Dennis W. Dickson[4] · Janice Robertson[5] · Kim A. Staats[6] · Justin K. Ichida[6] · Leonard Petrucelli[4] · Kendall Van Keuren-Jensen[3] · Rita Sattler[1]

Received: 14 September 2018 / Revised: 28 March 2019 / Accepted: 28 March 2019 / Published online: 3 April 2019

Abstract

The hexanucleotide repeat expansion GGGGCC $(G_4C_2)_n$ in the *C9orf72* gene is the most common genetic abnormality associated with amyotrophic lateral sclerosis (ALS) and frontotemporal dementia (FTD). Recent findings suggest that dysfunction of nuclear-cytoplasmic trafficking could affect the transport of RNA binding proteins in C9orf72 ALS/FTD. Here, we provide evidence that the RNA editing enzyme adenosine deaminase acting on RNA 2 (ADAR2) is mislocalized in C9orf72 repeat expansion mediated ALS/FTD. ADAR2 is responsible for adenosine (A) to inosine (I) editing of double-stranded RNA, and its function has been shown to be essential for survival. Here we show the mislocalization of ADAR2 in human induced pluripotent stem cell-derived motor neurons (hiPSC-MNs) from C9orf72 patients, in mice expressing $(G_4C_2)_{149}$, and in C9orf72 ALS/FTD patient postmortem tissue. As a consequence of this mislocalization we observe alterations in RNA editing in our model systems and across multiple brain regions. Analysis of editing at 408,580 known RNA editing sites indicates that there are vast RNA A to I editing aberrations in C9orf72-mediated ALS/FTD. These RNA editing aberrations are found in many cellular pathways, such as the ALS pathway and the crucial EIF2 signaling pathway. Our findings suggest that the mislocalization of ADAR2 in C9orf72 mediated ALS/FTD is responsible for the alteration of RNA processing events that may impact vast cellular functions, including the integrated stress response (ISR) and protein translation.

Keywords C9orf72 · ALS · FTD · Nucleocytoplasmic mislocalization · ADAR2 · RNA editing · RNA metabolism · iPSC neurons · RNA-seq · Neurodegeneration · Protein accumulation

Electronic supplementary material The online version of this article (https://doi.org/10.1007/s00401-019-01999-w) contains supplementary material, which is available to authorized users.

✉ Rita Sattler
Rita.Sattler@Dignityhealth.org

[1] Department of Neurobiology, Barrow Neurological Institute, 350 W Thomas Road, Phoenix, AZ 85013, USA

[2] School of Life Sciences, Arizona State University, Tempe, AZ, USA

[3] Neurogenomics Division, Translational Genomics Research Institute, Phoenix, AZ, USA

[4] Department of Neuroscience, Mayo Clinic Jacksonville, Jacksonville, FL, USA

[5] Tanz Centre for Research in Neurodegenerative Diseases, University of Toronto, Toronto, Canada

[6] Department of Stem Cell Biology and Regenerative Medicine, Eli and Edythe Broad Center for Regenerative Medicine and Stem Cell Biology, Keck School of Medicine, University of Southern California, Los Angeles, CA, USA

Introduction

Amyotrophic lateral sclerosis (ALS) is a fatal, neurodegenerative disorder caused by progressive loss of both upper and lower motor neurons, leading to muscle atrophy and eventually death due to respiratory failure [65]. A GGGGCC (G_4C_2) hexanucleotide repeat expansion (HRE) in the first intron of the *C9orf72* gene represents the most common genetic abnormality in ALS, as well as in frontotemporal dementia (FTD), to date [19, 53]. Extensive research on the role of the $(G_4C_2)_n$ repeat expansion in the *C9orf72* gene has led to the proposal of three alternative-but not mutually exclusive-pathogenic mechanisms: (1) protein loss-of-function [4, 8, 11, 17, 27, 58, 62, 66, 70], (2) toxic RNA gain-of-function [2, 21, 40, 41, 47, 54, 73], and (3) toxicity caused by repeat-associated non-AUG initiated (RAN) translation, which leads to the accumulation of dipeptide repeat proteins (DPRs) [3, 26, 37, 44, 46, 48, 63, 69, 71, 75, 76].

A more recent hypothesis suggests deficits in nucleocytoplasmic trafficking of mRNAs and/or proteins are caused by the repeat expansion in the *C9orf72* gene [9, 10, 24, 37, 70, 73]. Specifically, defects in nuclear protein import and nuclear mRNA export were observed in different models of C9orf72 disease, spanning human postmortem patient tissue, human induced pluripotent stem cell-differentiated neurons (hiPSC-neurons), drosophila, and yeast [10, 29]. In addition, several nuclear pore complex protein members were identified as genetic modifiers of C9orf72 disease pathogenesis [24, 37], or displayed aggregation at the nuclear membrane [73]. These findings strengthen the critical role of nucleocytoplasmic trafficking in neurodegenerative diseases and may explain why altered RNA metabolism is one of the major deficits described in C9orf72 disease pathogenesis.

Here, we show the nucleocytoplasmic mislocalization of the RNA binding protein, adenosine deaminase acting on RNA 2 (ADAR2), which we hypothesize leads to aberrant RNA processing in C9orf72 mediated ALS/FTD. ADAR2 is a member of the ADAR protein family, which deaminates adenosine in double-stranded RNA transcripts, thus catalytically converting a single nucleotide from an adenosine to an inosine (A-to-I) [5, 18, 38, 45]. ADAR2 is localized exclusively to the nucleus, and has been proposed to accumulate in the nucleus during neuronal development [6]. The catalytic conversion alters the hydrogen bonding capacity of the edited nucleotide and leads to recognition by cellular machinery as guanosine. ADAR1 and ADAR2 (commonly referred to as ADAR and ADARB1, respectively) are the two catalytically active proteins in the ADAR family and are highly regulated. Knockout of these proteins leads to epileptic-like seizures and death in mice, emphasizing its critical roles in normal brain development [34, 35, 67, 68]. ADAR3 (alternate nomenclature is ADARB2), while highly brain specific, is thought to be catalytically inactive and its role remains mostly unknown [13] (see also Online Resource 1).

Although RNA editing deficits are believed to play an important role in neurodegeneration, there have been relatively few studies investigating A to I editing in disease. Previously, studying RNA editing was difficult and relied on the serendipitous discovery of A to I editing sites [42, 61]. The increasing ease and availability of RNA sequencing allow for more robust characterization of A to I RNA editing using a more quantitative method. These RNA-seq based approaches look for mismatched pairing in the transcriptome to the genome allowing for analysis of every RNA editing site in the transcriptome [61]. Utilizing these methods, there have been millions of A to I RNA editing sites reported, suggesting it may be one of the most common post-transcriptional modifications [23, 42, 61]. While the function of a few of these RNA editing events are well characterized such as the GluA2 Q/R site, the A-E sites of the 5HT-2C serotonin receptor, or the Kv1.1 potassium channel, the large majority of RNA editing events have an unknown impact on cellular function [42, 72]. Nevertheless, dysregulation of crucial post-transcriptional modifications of editing target genes have been associated with sporadic ALS, Alzheimer's disease, Huntington's disease, Parkinson's disease, epilepsy, stroke, as well as many types of cancer [12, 42, 56, 57]. Interestingly, a recent study showed widespread RNA editing changes in postmortem autopsy brain tissue from persons with autism spectrum disease (ASD), as well as brains from individuals with Fragile X syndrome, supporting the broad hypothesis that RNA editing dysregulation will uncover novel mechanisms of neurological, neurodegenerative and/or neuropsychiatric diseases.

To thoroughly assess the cytoplasmic mislocalization of ADAR2 in C9orf72 ALS/FTD, we examined varying brain regions of human postmortem C9orf72 patient tissue, C9orf72 patient-derived hiPSCs differentiated into motor neurons (hiPSC-MNs), and wild type (WT) mice expressing $(G_4C_2)_{149}$ by means of somatic brain transgenesis using adeno-associated virus (AAV) vectors [16]. Fluorescent immunolabeling of ADAR2 protein revealed aberrant ADAR2 staining in the neuronal cytoplasm of C9orf72 ALS/FTD patient postmortem spinal cord and motor cortex tissue, C9orf72 ALS/FTD hiPSC-MNs, and different brain regions of AAV9-$(G_4C_2)_{149}$-transduced WT mice. Interestingly, ADAR2 showed no alterations in gene expression levels in C9orf72 ALS/FTD, in comparison to what had been found in sporadic ALS spinal cord motor neurons [33]. To study the functional consequence of the mislocalization of ADAR2, we utilized RNA sequencing of patient tissue and differentiated hiPSC-MNs to analyze the whole transcriptome for RNA A to I editing changes. We uncovered widespread RNA editing aberrations (hypo- and hyperediting) in varying brain regions of C9orf72 ALS/FTD patient tissue as well as C9orf72 patient hiPSC-MNs. These RNA alterations were assigned to 1,526 genes, including genes involved in ALS related transcripts and the EIF2 signaling pathway. These data provide new insights into the contribution of RNA A to I editing in neurodegeneration caused by the C9orf72 repeat expansion. In addition, these data demonstrate functional consequences of C9orf72 HRE-mediated nucleocytoplasmic trafficking defects, supporting the critical role of functional trafficking of RNA processing proteins between the cytoplasm and nucleus.

Methods

AAV9-(G_4C_2) over expressing mouse tissue

AAV9-$(G_4C_2)_2$ and AAV9-$(G_4C_2)_{149}$ injected mouse brain sections were generously provided by Dr. Leonard Petrucelli. Mice were generated as previously described [16,

74]. All procedures using mice were performed in accordance with the National Institutes of Health Guide for Care and Use of Experimental Animals and approved by the Mayo Clinic Institutional Animal Care and Use Committee (Mayo Clinic protocol numbers A42014 and A47214).

Cloning of full length-ADAR2 and ΔNLS-ADAR2 constructs

ADAR2-pEZ-Lv111 (GeneCopoeia #U73197-pEZ-EX-Y2482-Lv111) lentiviral clone was used as a starting point for the generation of FL-ADAR2, ΔNLS-ADAR2, and empty vector plasmids. The original clone was linearized by NheI-HF and XbaI (NEB- R3131S, R0145S) double digest, gel purified (Zymo Research-D4008) and ligated (NEB-M2200S) to create empty vector. FL-ADAR2 and ΔNLS-ADAR2 plasmids were created using the NEBuilder HiFi DNA Assembly Cloning Kit (NEB-E2621S), with ADAR2-pEZ-Lv111 destination vector linearized with XbaI and Bsu36I (NEB-R0524S) and gel purified. Fragments were amplified via PCR (Thermo Scientific-F549S) using ADAR2-pEZ-Lv111 as a template for the following primer combinations: FL-ADAR2, 5′-ACC TCCATAGAAGATTCTAGAGCCACCATGGATATA GAAGACGAAGAGAATATGAGTTCC-3′ and 5′-GGG AAACTGGACAAAATACCTCAG-3′; ΔNLS-ADAR2 fragment 1,5′-ACCTCCATAGAAGATTCTAGAGCC ACCATGGATATAGAAGACGAAGAGAATATGAGT TCC-3′ and 5′-AGAACGGGCCCTGGTGTGCTGGTG CTACCACCACCCAGG-3′, and fragment 2,5′-ACACCA GGGCCCGTTCT-3′ and 5′-GGGAAACTGGACAAAATA CCTCAG-3′. Prior to HiFI assembly, PCR products were spin-column purified (Promega-A9282).

Human induced pluripotent stem cell-derived motor neuron RNA sequencing

Four C9orf72 ALS/FTD and three control hiPSC motor neuron lines were lysed using QIAshredder (QIAGEN-79654) and RNA was isolated with RNeasy Mini Kit (QIAGEN-74104). Isolated RNA was quantified using Quant-iT Ribogreen RNA Assay (ThermoFisher-R11490). Double-stranded cDNA libraries were synthesized from 10 ng total RNA with RIN value of 6 or better using SMARTer Stranded Total RNA-Seq Kit v2-Pico Input (Takara Bio-634413). Libraries were combined into equimolar pools and sequenced on an Illumina paired-end flowcell (Illumina-PE-401-3001) with a 1% v/v Phix v3 spike-in (Illumina-FC-110-3001) on Illumina's HiSeq 2500 with TruSeq v3 chemistry (Illumina-FC-401-3002). The first and second reads were 82 base pairs in length.

Human tissue RNA sequencing

All human tissue RNA sequencing was performed by Target ALS (http://www.targetals.org/) in collaboration with the New York Genome Center. All sequencing data including methods and quality controls are publicly available at: https://metronome.nygenome.org/TargetALS/.

Immunocytochemistry

Cells were fixed using 4% paraformaldehyde (PFA; EMS-15714-S) for 30 min at room temperature, permeabilized with 0.1% Triton X-100 then blocked with 1% Bovine Serum Albumin (BSA; Sigma-05470) and 10% Normal Goat Serum (NGS; Vector-S1000) for 1 h. Cells were incubated with primary antibodies overnight at 4 °C in phosphate buffered saline (PBS) containing 1% BSA and 10% NGS. Primary Antibodies included anti-MAP2 (Synaptic Systems-188 009) 1:1000 and anti-ADAR2 (Sigma-HPA018277) 1:500. Next, cells were washed in PBS three times for 5 min each and incubated with Alexa Fluor 555 (Intivrogen-A21429) 1:750 and Alexa Fluor 633 (Invitrogen-A21105) 1:200 in PBS with 1% BSA and 10% NGS for 2 h at room temperature. Cells were then washed with PBS three times for 5 min each and mounted using prolong antifade gold with DAPI (Life Technologies-P36930). Cells were imaged on a Zeiss LSM800 laser scanning confocal microscope using Plan Apochromat 63× oil immersion objectives. Z-Stack images were acquired using identical laser settings and normalized within a given experiment.

Immunohistochemistry

Mouse AAV9-$(G_4C_2)_2$ and AAV9-$(G_4C_2)_{149}$ as well as C9orf72 ALS/FTD and non-ALS control patient post mortem spinal cord, motor cortex, and frontal cortex were paraffin embedded and sectioned into 10 µm sections. Sections were heated to 60 °C for 30 min and de-paraffinized in three separate 10 min Clearrite (Thermo-6901) washes. Sections were dehydrated in subsequent 95% and 100% ethanol washes and rehydrated in dH_2O. Antigen retrieval was then performed in Dako epitope retrieval solution pH 9.0 (Dako-S2368) for 35 min in a steamed chamber. Next cool running dH_2O was rinsed over the tissue for 10 min to remove epitope retrieval solution. Sectioned tissue was blocked at room temperature for 1 h in Dako blocking solution (Dako-X0909). Sections were then incubated in antibody dilutant (Dako-S3022) solution containing, anti-ADAR2 (sigma-HPA018277) 1:500 primary antibody for 16 h at 4 °C in humified chamber. Mouse and human sections were washed three times for 5 min each in PBS then incubated in Dako antibody dilutant with 1:750 Alexa Fluor 555 (Intivrogen-A21429) secondary antibody for 1 h at room temperature.

The tissue sections were then washed three times in PBS for 5 min and blocked in Dako blocking solution for 1 h at room temperature. This was followed by incubation in Dako antibody dilutant solution containing anti-MAP2 (Synaptic Systems-188 009) 1:1000 primary antibody for 16 h at 4 °C in humified chamber. Next sections were washed three times for 5 min each in PBS and incubated in Dako antibody dilutant with Alexa Fluor 633 (Invitrogen-A21105) 1:200 secondary antibody for 1 h at room temperature. The tissue sections were then washed three times in PBS for 5 min and mounted using prolong antifade gold with DAPI (Life Technologies-P36930). Tissue sections were imaged on a Zeiss LSM800 laser scanning confocal microscope using Plan Apochromat 63× oil immersion objectives. Z-Stack images were acquired using identical laser settings and normalized within a given experiment. Basic clinical and demographic data from human postmortem tissue utilized is available in Online Resource 2.

Image analysis

Images were processed using Imaris software. The nucleocytoplasmic ratio of ADAR2 was calculated as previously described [73]. Briefly, the cytoplasm via MAP2 (Synaptic Systems-188 009) labeling and the nucleus via DAPI (Life Technologies-P36930) labeling were designated as distinct regions of interest at each Z-plane in an image. Pixel intensity per μm^3 was used to generate nucleocytoplasmic ratios. ADAR2 Nucleocytoplasmic Ratios were calculated for 200 C9orf72 ALS/FTD and control hiPSC-MNs. *t*-Tests were performed in graphpad prism v 7.04 to determine significance ($p < 0.05$), $n = 200$ neurons per group.

Induced pluripotent stem cell differentiation

C9orf72 ALS/FTD and healthy control hiPSC colonies were grown and cultured in 10 cm Matrigel (Corning-356235) coated dishes with mTeSR1 (Stem Cell Technologies-85850) media supplemented with ROCK inhibitor (Stem Cell Technologies-72304). Partially differentiated, or spontaneously differentiated cells were manually removed before differentiation began. Neuralization was induced over 2 days using WiCell Medium (DMEM/F12, knockout serum replacement, 1% L-glutamine, 1% NEAA, 110 µM 2-mercaptoethanol + 0.5 µM LDN-193189 (Stemgent-04-0074-02) + 10 µM SB431542 (Stemgent-04-001-05) for Bone Morphogenetic Protein and SMAD pathway inhibition. During caudalization cells were cultured in equal parts WiCell and neural induction medium (NIM:DMEM/F12, 1% L-glutamine, 1% NEAA, 1% N2, 1% Pen/Strep and 2 µg/mL heparin) + 0.5 µM LDN, 10 µM SB and 0.5 µM retinoic acid (RA:Sigma-R2625). Ventralization was induced by culturing cells for 7 days in NIM + 0.5 µM RA, 200 ng/mL purmorphamine (EMD Millipore-540220) + 10 ng/mL Brain-Derived Neurotrophic Factor (BDNF: Stem Cell Technologies-78005) + 0.4 µg/mL Ascorbic Acid (ASAC: MP-Biomedical-194586). Next, during the neural progenitor stage the cells were cultured in equal parts NIM and neural differentiation media (NDM; Neurobasal, 1% L-glutamine, 1% NEAA, 1% N2, 1% Pen/Strep) + 0.5 µM RA + 200 ng/mL purmorphamine + 0.4 µg/mL ASAC + 2% B27 (Gibco-17504044) + 10 ng/mL BDNF + 10 ng/mL Glial cell line-Derived Neurotrophic Factor (GDNF: Stem Cell Technologies-79058) + 10 ng/mL Insulin-like Growth Factor 1 (IGF-1: Stem Cell Technologies-78022) + 10 ng/mL Ciliary Neurotrophic Factor (CNTF: Stem Cell Technologies-78010) for 6 days. For the remainder of the differentiation, cells were cultured and maintained in NDM + 0.5 µM RA + 200 ng/mL purmorphamine + 0.4 µg/mL ASAC + 2% B27 + 10 ng/mL BDNF + 10 ng/mL GDNF + 10 ng/mL IGF + 10 ng/mL CNTF. At 32 days in vitro (DIV) cells were treated with 20 nM Cytosine β-D-arabinofuranoside (Sigma-C1768) for 48 h to remove glial progenitors and enrich for hiPSC neurons. For immunofluorescence experiments, DIV 40 neurons were co-cultured on top of a confluent monolayer of mouse astrocytes. Cells were kept alive until DIV 60–65 and then fixed for immunofluorescence. For RNA sequencing experiments, cells were not plated on mouse astrocytes to enrich for hiPSC neuronal RNA. Basic clinical and demographic data from hiPSC lines utilized is available in Online Resource 2.

Lentivirus production and HEK cell transduction

FL-ADAR2, ΔNLS-ADAR2 and, empty vector control plasmids were each combined with the packaging, pMD2.G, and envelope, psPAX2, plasmids (gifts from Didier Trono; Addgene-12259), and were transformed into One Shot Stbl3 Chemically Competent *E. coli* (Invitrogen-C737303). Plasmid DNA was prepared using Qiagen's Maxi Kit recommendations for low-copy plasmid (Qiagen-12162). Plasmid concentration for transfection applications was measured with NanoDrop (Thermo Scientific-ND2000). Prior to transfection, HEK 293T cells were plated on 15 cm poly-L-lysine (Sigma-355482) coated dishes, seeded at a density of 10×10^6 cells, and grown to confluency in DMEM (Gibco-11995-065) + 10% FBS (Hyclone-SH3007003IH). Lentiviral vectors were generated via transient cotransfection of HEK 293T cells using a second generation, three-plasmid system. Transfer vector plasmid (8 µg), envelope plasmid (16 µg), and packaging plasmid (4 µg) DNA were mixed together in 1 mL OptiMEM (Gibco-11058021) prior to the addition of linear polyethylenimine (PEI: Polysciences, Inc-23966-1) at a ratio of 3:1 (PEI:DNA) [52]. Media was changed 5 h after transfection and lentivirus harvested 24, 48, and 72 h later using the Lenti-X Concentrator (Clontech-631231) protocol.

HEK293 cells were transduced for 48 h and expression was quantified using SDS-PAGE followed western blot analysis with anti-ADAR2 (sigma-HPA018277) 1:500 primary antibody for 16 h rocking at 4 °C.

Postmortem human tissue

De-identified postmortem control and C9orf72 ALS/FTD and AD patient spinal cord, motor cortex, or frontal cortex were obtained from the Target ALS human postmortem Tissue core, Dr. Elliott Mufson, Barrow Neurological Institute and from Dr. Janice Robertson, University of Toronto, Canada. ALS cases were diagnosed using the Revised El Escorial Criteria, and patient consents were obtained in accordance with institutional ethical review boards. Control and ALS cases were processed using the same procedures and were genotyped for common ALS genes. Basic clinical and demographic data of postmortem human tissue is available in Online Resource 2.

siRNA treatments

Day 65 hiPSC differentiated motor neurons were target for specific knockdown for ADAR1, ADAR2, or both ADAR 1 and 2 using a pool of 4 siRNAs (Accell, Dharmacon). siRNA treatments were kept on the cells for 5 days before the neurons were lysed with a QIAshredder (QIAGEN-79654) and RNA was isolated with an RNeasy Mini Kit (QIAGEN-74104).

RNA editing analysis and statistics

Calculation of the 408,580 RNA editing ratios was performed as previously described [61]. Briefly, editing levels at each site were quantified by dividing the number of guanosine reads by the sum of guanosine and adenosine reads. To limit false representation of editing sites due to low read counts, we only included editing calculations for sites that had at least 20× coverage in tissue and 5× coverage in cells. In addition, at least half of the total samples in both C9orf72 ALS/FTD samples and non-ALS control samples had to have coverage at each site. The total number of sites that fit these criteria were: 28,891 sites in the cerebellum, 32,801 sites in the frontal cortex, 26,022 sites in the motor cortex, 39,425 sites in the lumbar spinal cord, and 6777 sites in hiPSC motor neurons had the quality and coverage to meet these criteria (Online Resource 3). We then calculated RNA editing ratios at each of these sites in C9orf72 ALS/FTD and non-ALS controls. As described previously fishers exact test was performed in base R v. 3.5.1 to each site that met our criteria [64]. We performed Bonferroni corrections to adjust for false discovery rate. Most editing sites did not have a significant p value after adjustment (see Online Resource 3). To have enough sites for analysis, and to explore the effects of ADAR2 mislocalization on editing, we utilized editing sites with unadjusted p value < 0.05 for downstream analysis. We utilized the R package biomaRt v. 2.36.1 to align the RNA editing sites with the human transcriptome (GRCh37) to call their gene names. The canonical pathways related to RNA editing aberrations were generated through the use of IPA (QIAGEN Inc., https://www.qiagenbioinformatics.com/products/ingenuity-pathway-analysis). Basic Clinical and demographic data on samples utilized for RNA editing analysis are available in Online Resource 2.

RNA sequencing analysis

FASTQ files from hiPSC motor neuron RNA sequencing and the NYGC were aligned to the human genome (GRCh37) using STAR v. 2.5.3a. Raw gene counts were determined from BAM files using FeatureCounts v. 1.5.3. Transcripts per Million (TPMs) were calculated from aligned BAM files using Salmon v. 0.8.0. Using these TPMs, we calculated the average gene expression for *GluA1-4* and *ADAR1-3* in C9orf72 ALS/FTD and non-ALS hiPSC samples and performed t-tests to determine significance ($p < 0.05$). We calculated fold changes in disease compared to control to understand gene expression changes.

Results

Nucleocytoplasmic mislocalization of ADAR2 in C9orf72 HRE-mediated ALS/FTD in vitro and in vivo

We and others have previously shown that the C9orf72 HRE leads to nucleocytoplasmic trafficking deficits, which greatly affects the localization of RNA binding proteins such as TDP-43 [73]. ADAR2 contains a nuclear localization sequence (NLS) and is located within the nucleus under physiological conditions where it can interact with and edit pre-mRNA [42]. We first examined C9orf72 ALS/FTD patient postmortem spinal cord tissue samples for ADAR2 mislocalization using standard immunohistochemistry techniques. As predicted, ADAR2 was detected predominantly in the nucleus in the anterior horn of non-ALS control spinal cord (Fig. 1a–c). However, the anterior horn of C9orf72 ALS/FTD patient spinal cord exhibited strong cytoplasmic accumulations and aggregations of ADAR2 (Fig. 1d–f; see also Online Resource 4a, b). Quantification of ADAR2 localization in MAP2 positive neurons revealed that 15.3% of control MNs showed a cytoplasmic presence of ADAR2, while 42.3% ($p = 0.039$, t-test) of C9orf72 spinal motor neurons have aberrant ADAR2 protein expression patterns (Fig. 1g). Due to

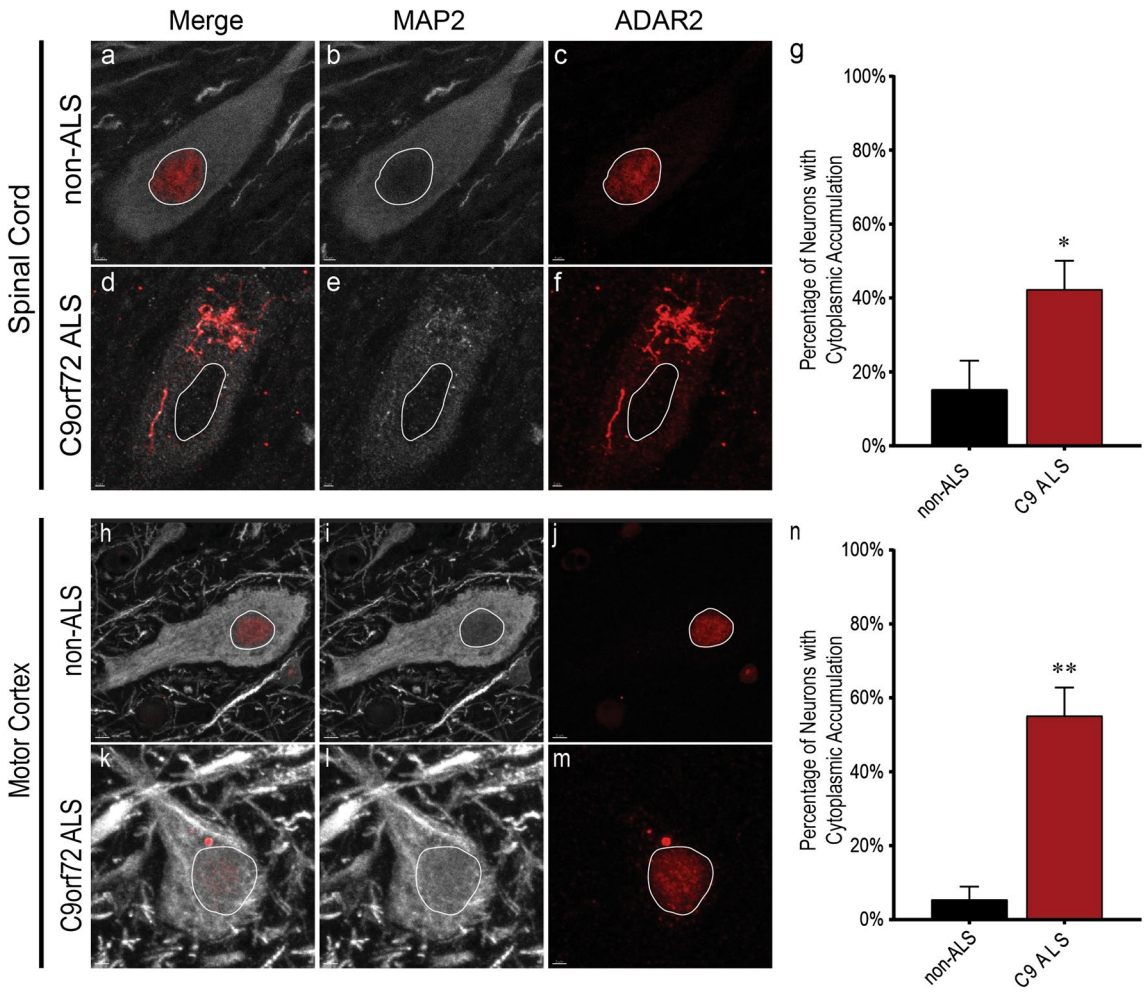

Fig. 1 ADAR2 is mislocalized in C9orf72 ALS/FTD patient spinal cord and motor cortex. **a**–**c** MAP2 positive neuron showing normal ADAR2 localization from the anterior horn of a non-neurological control spinal cord. **d**–**f** MAP2 positive neuron with aberrant ADAR2 accumulation in the cytoplasm from the anterior horn of C9orf72 ALS/FTD patient spinal cord. **g** Percent of total MAP2 positive spinal motor neurons that exhibit ADAR2 cytoplasmic accumulation (*$p = 0.039$, *t*-test). **h**–**j** MAP2 positive neuron showing normal ADAR2 localization from the motor cortex of a non-neurological control patient. **k**–**m** MAP2 positive neuron showing mislocalized ADAR2 in the cytoplasm from the motor cortex of a C9orf72 ALS/FTD patient. **n** Percent of total MAP2 positive neurons in C9orf72 ALS/FTD motor cortex that exhibit ADAR2 cytoplasmic accumulation (**$p = 0.001$, *t*-test)

skein-like inclusions of ADAR2, we wondered if there was co-occurrence of mislocalization with TDP-43. Indeed, while low in occurrence, a significant number of neurons exhibited ADAR2 cytoplasmic accumulation together with TDP-43 pathology in C9orf72 ALS/FTD patient spinal cord (Online Resource 5a–i). Additionally, ADAR2 cytoplasmic accumulations can be occasionally detected in the dendrites of motor neurons in C9orf72 ALS/FTD patient spinal cord (Online Resource 4c–e). ADAR2 was also found to be significantly mislocalized in the motor cortex of C9orf72 ALS/FTD postmortem patient tissue where 55.1% ($p = 0.001$, *t*-test) of MAP2 positive neurons exhibit cytoplasmic accumulation of ADAR2 (Fig. 1h–n; see also Online Resource 6). C9orf72 ALS/FTD frontal cortex did not exhibit significant mislocalization of ADAR2, but 24.0% ($p = 0.1$, *t*-test) of MAP2 positive neurons did display cytoplasmic accumulation of ADAR2 (Online Resource 7).

To further our understanding of the localization of ADAR2, we wondered whether the nucleocytoplasmic mislocalization of ADAR2 is also found in C9orf72 patient-derived hiPSC-MNs. We immunolabeled hiPSC-MNs on day 55 of differentiation for ADAR2 and similar to healthy control spinal cord, ADAR2 is found predominantly in the nucleus of hiPSC-MNs from healthy control subjects (Fig. 2a–d), while C9orf72 hiPSC-MNs showed significant cytoplasmic accumulation of ADAR2, similar to what we discovered in C9orf72 ALS/FTD patient tissue (Fig. 2e–i; see also Online Resource 8). Quantification of the fluorescence intensities of the two compartments using Imaris

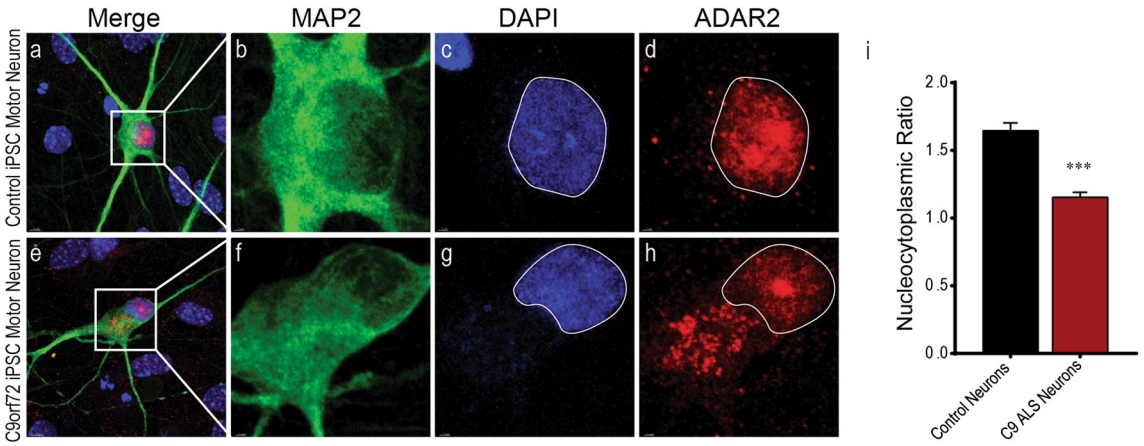

Fig. 2 ADAR2 is mislocalized in C9orf72 ALS/FTD patient-derived hiPSC motor neurons. **a**–**d** ADAR2 localized primarily in the nucleus of a healthy control MAP2-positive hiPSC-MN. **e**–**h** Aberrant ADAR2 accumulation in the cytoplasm of a MAP2 positive hiPSC-MN from a C9orf72 ALS/FTD patient. **i** Nucleocytoplasmic ratio of ADAR2 in control hiPSC motor neurons and C9orf72 ALS/FTD derived motor neurons (***$p < 0.005$, *t*-test)

image analysis reveals a significant decrease in the nucleocytoplasmic ratio of ADAR2 in C9orf72 ALS/FTD hiPSC-MNs (Fig. 2i; $p < 0.0001$).

Next, we looked for ADAR2 mislocalization in an in vivo model of C9orf72 ALS/FTD disease. The C9orf72 ALS/FTD mouse model utilizing an AAV9 overexpression of a $(G_4C_2)_2$ and $(G_4C_2)_{149}$ repeat expansion was generously provided by Dr. Leonard Petrucelli [16, 74]. At 6 months of age, $(G_4C_2)_2$ control mice showed distinct nuclear ADAR2 expression in frontal cortex (Fig. 3a, d), motor cortex (Fig. 3e, h), and hippocampus (Fig. 3i, l) with little evidence of cytoplasmic accumulation. However, $(G_4C_2)_{149}$ overexpressing mice exhibited significant cytoplasmic accumulations of ADAR2 in motor cortex (Fig. 3q, t, y; $p = 0.0064$) and hippocampus (Fig. 3u, x, aa; $p = 0.045$) as well as increased cytoplasmic ADAR2 accumulations in frontal cortex (Fig. 3m, p, z; $p = 0.06$).

Since the discovery of nucleocytoplasmic trafficking defects in C9orf72 ALS/FTD, other neurodegenerative diseases were found to exhibit similar dysfunction, including Huntington's disease [25, 28], Alzheimer's disease (AD) and tau-mediated FTD [22, 50]. We, therefore, examined select non-ALS postmortem brain tissue from AD patients with varying degrees of dementia. We identified cytoplasmic ADAR2 accumulations in the frontal cortex of 20.3% ($p = 0.49$) of neurons in patients with mild cognitive impairment and in 21.5% ($p = 0.43$) of neurons in patients with mild AD. When we stained postmortem tissue from severe AD patients, a significant number of neurons showed distinct cytoplasmic ADAR2 localization (39.66%; $p = 0.04$) (see Online resource 9).

These results support the notion that ADAR2 mislocalization is a downstream event of nucleocytoplasmic trafficking defects observed in C9orf72 ALS/FTD, but also other neurodegenerative diseases characterized by nuclear pore defects. What triggers these trafficking deficits likely differs among these diseases and is still largely unknown.

ADAR2 expression levels are unchanged in C9orf72 ALS/FTD patient postmortem tissue and hiPSC motor neurons

Previous studies in sporadic ALS showed decreased ADAR2 expression in laser captured spinal motor neurons of ALS patients [32]. We, therefore, analyzed existing RNA sequencing data for changes in gene expression of all members of the ADAR family. The New York Genome Center (NYGC), in collaboration with the Target ALS consortium has performed RNA sequencing on postmortem brain and spinal cord tissue samples of ALS patients irrespective of etiology and has made these data publicly available for researchers worldwide. Using normalized RNA transcript per million from these data sets, we compared gene expression fold changes of *ADAR1-3* in spinal cord, motor cortex, frontal cortex and cerebellum between C9orf72 ALS/FTD patients and healthy controls (Online Resource 10). Interestingly, *ADAR1* expresses slightly higher in C9orf72 ALS/FTD cerebellum (Fold Change (FC) = 1.14, $p = 0.01$, *t*-test). No changes were observed for any other members of the *ADAR* family (*ADAR1-3*) in any of the other analyzed brain regions. This discrepancy to the prior studies described above could be due to reduced specificity in the bulk RNA sequencing approach. To look at individual motor neurons, we performed RNA sequencing on C9orf72 ALS/FTD patient-derived hiPSC motor neurons, which do show significant ADAR2 mislocalization as shown in Fig. 2. RNA sequencing from these cells confirmed the results obtained from human postmortem spinal cord tissues

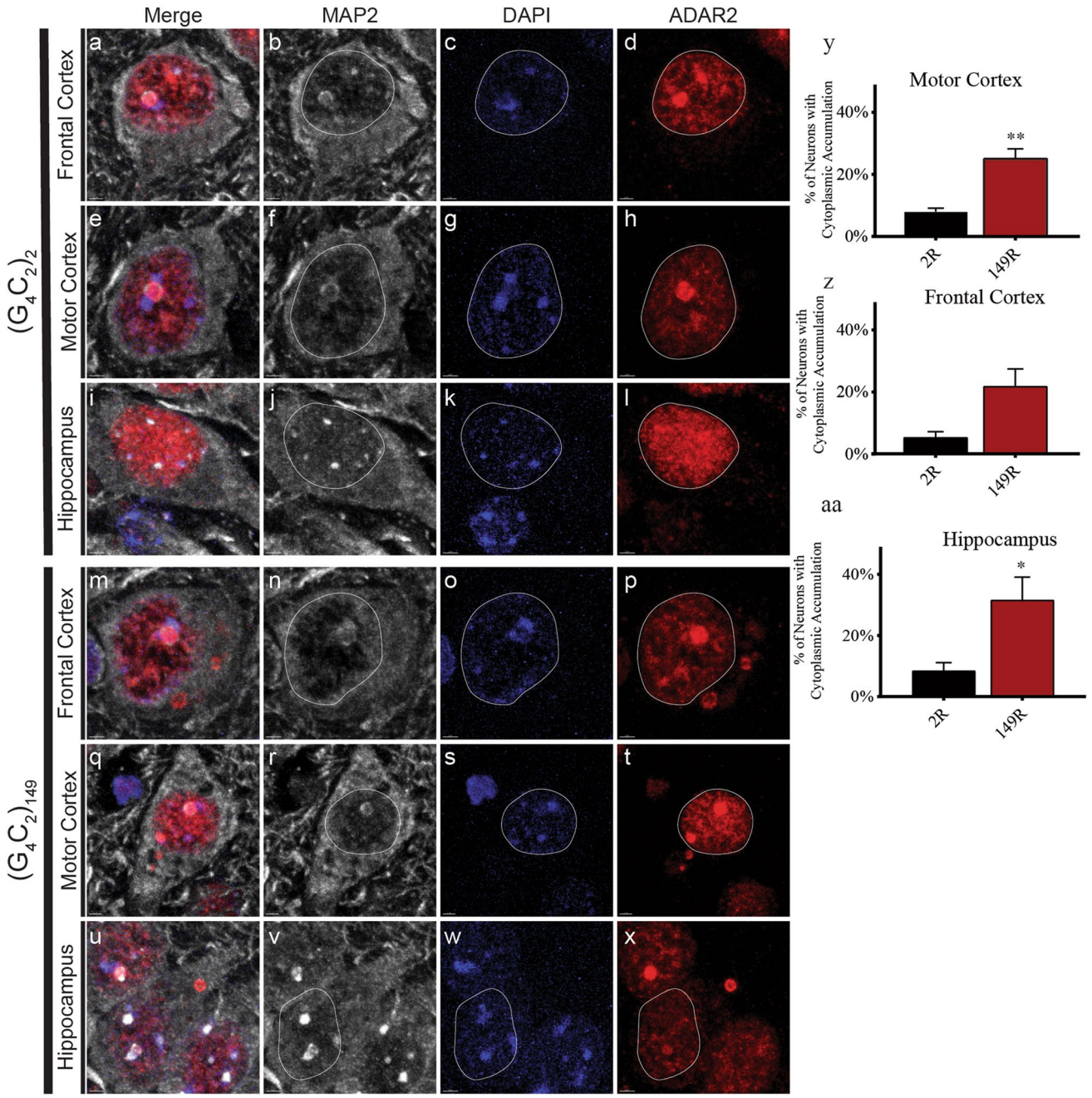

Fig. 3 ADAR2 is mislocalized in mice expressing $(G_4C_2)_{149}$. ADAR2 staining is nuclear in the **a**–**d** frontal cortex, **e**–**h** motor cortex, and **i**–**l** hippocampus in 6 month old control mice expressing a $(G_4C_2)_2$ hexanucleotide repeat. Cytoplasmic accumulations of ADAR2 are found in the **m**–**p** frontal cortex, **q**–**t** motor cortex, and **u**–**x** hippocampus in 6 month old disease mice expressing a $(G_4C_2)_{149}$ hexanucleotide repeat. Quantification of total MAP2 positive neurons that showed cytoplasmic ADAR2 accumulation in the **y** motor cortex ($p = 0.0064$), **z** frontal cortex ($p = 0.06$), and **aa** hippocampus ($p = 0.045$, *t* test)

showing no gene expression changes in the three *ADAR* genes (*ADAR1*; FC = 1.30, $p = 0.980$; *ADAR2*, FC = 0.85, $p = 0.9622$; *ADAR3*, FC = 1.20, $p = 0.883$, *t*-tests). Given the critical function of ADAR2 editing on AMPA receptor subunit GluA2 and its relevance in sporadic ALS, as well as the recent findings of increased levels of *GRIA1* in C9orf72 ALS/FTD hiPSC-MNs [55, 58], we also examined gene expression levels of all AMPA receptor subunits (GluA1-4/*GRIA1-4*). No gene expression level changes were observed in the AMPA receptor subunits across all brain regions including spinal cord and hiPSC motor neurons (Online Resource 10).

RNA A to I editing aberrations in C9orf72 ALS/FTD

Our data provide evidence that the RNA editing protein ADAR2 is mislocalized in C9orf72 ALS/FTD patient tissues and C9orf72 disease models, both in vitro and in vivo. To characterize alteration in ADAR2 function as a result of its cytoplasmic accumulation in C9orf72 ALS/FTD, we interrogated the RNA sequencing data sets for transcriptome-wide changes in RNA A to I editing. We utilized a mammalian RNA editing reference atlas consisting of 408,580 A to I editing sites across the entire transcriptome as previously described [61]. We applied cutoffs to prevent artifacts due to low sequencing read counts and required that each site had at least 20× coverage in at least half the non-ALS control samples and half the C9orf72 ALS/FTD samples. After this filtering, we identified 28,891, 32,800, 26,021 and 39,435 known A to I editing sites in the cerebellum, frontal cortex, motor cortex and lumbar spinal cord, respectively, and 6777 sites in hiPSC motor neurons (Online Resource 3). Comparison of A to I editing ratios at these editing sites yielded 11,466 aberrantly editing RNA editing sites spanning 1458 genes (Online Resource 3). A to I editing sites in C9orf72 ALS/FTD postmortem tissue were compared to non-ALS control tissue and were determined to be differentially edited as previously described [64] using fishers-exact test ($p < 0.05$). We used Bonferroni corrections to adjust for false discovery rate. Most editing sites did not have a significant p-value after adjustment (see Online Resource 3). To have enough sites for analysis, and to explore the effects of ADAR2 mislocalization on editing, we utilized editing sites with unadjusted p value < 0.05 for downstream analysis. With these criteria, C9orf72 ALS/FTD spinal cord tissue alone exhibited 3814 RNA editing aberrations across 902 genes (Fig. 4a–c, Online Resource 3). Additionally, we detected 2792, 2680 and 2180 A to I editing aberrations in cerebellum, frontal cortex and motor cortex, respectively (Fig. 4d–f, Online Resources 3, 11). We did not observe total changes in RNA editing in any of the individual brain regions analyzed (spinal cord: Ctrl 6.1%; C9 6.04%; motor cortex: Ctrl 6.26%, C9 6.02%; frontal cortex: Ctrl 5.92%, C9 5.92%; cerebellum: Ctrl 7.20, C9 7.50). We performed unsupervised hierarchical clustering on RNA editing analysis, which resulted in the segregation of C9orf72 ALS/FTD spinal cord (Fig. 4a, red) and non-ALS control spinal cord

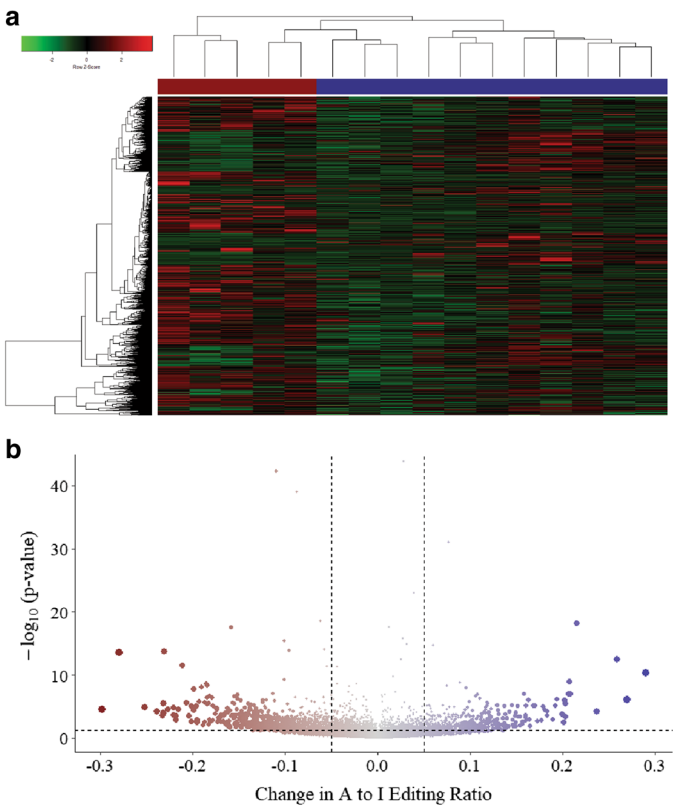

c

C9orf72 ALS/FTD Spinal Cord	
Gene	Percentage Change
KIDINS220	-28.93
CHD2	-26.87
ANKRD18A	-25.88
OSBPL9	-23.66
NDRG4	-23.23
ATG14	23.16
MCUR1	23.93
SNRPD3	25.23
PLXDC2	28.06
ARSD	29.85

d

C9orf72 ALS/FTD Motor Cortex	
Gene	Percentage Change
NDRG4	-38.01
LINC-PINT	-24.10
MGEA5	-23.57
TMEM165	-23.42
CLASP2	-22.15
SORBS1	19.76
MRPL19	19.91
FZD3	20.48
SMAD9	20.52
SORBS1	35.15

e

C9orf72 ALS/FTD Frontal Cortex	
Gene	Percentage Change
NDRG4	-24.22
LINC-PINT	-18.86
RTN4	-16.49
RICTOR	-16.42
ARPP21	-16.41
SFXN1	13.68
DCAF16	13.94
DENND3	14.39
UCHL1	18.37
KCNJ6	19.94

f

C9orf72 ALS/FTD Cerebellum	
Gene	Percentage Change
RICTOR	-23.85
NDRG4	-17.79
RTN4	-17.16
ALS2	-16.73
KATNBL1	-16.19
ZNF844	16.64
SGPP2	16.75
LINC01004	18.96
CPSF3L	19.37
LINC-1004	20.77

Fig. 4 Widespread adenosine to inosine RNA editing aberrations in C9orf72 ALS/FTD. **a** Unsupervised hierarchical clustering distinguishes between C9orf72 ALS/FTD and control groups based on editing ratios. **b** Volcano plot depicting widespread RNA editing aberrations in C9orf72 ALS/FTD postmortem tissue where 3814 A to I editing sites are significantly ($p < 0.05$, Fisher's exact test) misedited in C9orf72 ALS/FTD spinal cord. List of most highly misedited genes that exhibit increased editing (blue) and decreased editing (red) relative to controls in C9orf72 ALS/FTD **c** spinal cord, **d** motor cortex, **e** frontal cortex, and **f** cerebellum

tissue (Fig. 4a, blue). These data suggest similar RNA editing profiles in different patient samples of C9orf72 ALS/FTD spinal cord postmortem tissue. These editing alterations are prone to both hyper- and hypo-editing alterations (Fig. 4b). To highlight the most dysregulated editing sites we provided tables listing absolute changes of the most dysregulated genes in C9orf72 ALS/FTD spinal cord (Fig. 4c), motor cortex (Fig. 4d), frontal cortex (Fig. 4e), and cerebellum (Fig. 4f). Additionally, we have observed robust RNA editing alterations in C9orf72 ALS/FTD hiPSC-MNs where 5540 differentially edited sites impact 1612 genes (Online Resource 12). A complete list of differentially edited sites and genes, including absolute and relative A to I RNA editing changes, is provided in Online Resource 3. To categorize the editing aberration sites, we utilized the genomic locations of each differentially edited A to I site in C9orf72 ALS/FTD disease tissue and classified the editing aberrations using the ensemble CRCh37 Variant Effect Predictor (Online Resource 13). Not surprisingly, the majority (~99%) of sites altered in C9orf72 ALS/FTD are in non-coding, intronic, and gene-regulatory elements, suggesting that gene alterations such as alternative splicing or overall gene expression are likely to be affected by the editing dysfunction. The hypothesized evolutionary role of ADAR mediated A to I editing is the regulation of the retrotransposition of *Alu* repetitive elements [49]. Dysregulation of retrotransposons have been shown to increase with aging as well as induce a neurodegenerative phenotype in AD models [59], suggesting that dysregulation of retrotransposons could play a role in C9orf72 disease pathogenesis.

ADAR2 siRNA treatment simulates RNA A to I editing aberrations in hiPSC-MNs

To elucidate if the editing aberrations found in C9orf72 ALS/FTD were triggered by a loss of editing function of ADAR2 we treated hiPSC-MNs with siRNAs targeted to ADAR2, ADAR1 or both. Reduction of ADAR1 levels resulted in 4289 hypo-edited sites and 631 hyper-edited sites and ADAR2 siRNA treatment lead to 3035 hypo-edited sites and 866 hyper-edited sites (Online Resource 14). Knock down of both ADAR1 and ADAR2 resulted in 4217 hypo-edited sites and only 447 hyper-edited sites (Online Resource 14). These data suggest that ADAR1 might be compensating at some editing sites for the loss of function of ADAR2 in C9orf72 disease, in some instances even above baseline editing levels, thereby leading to hyper-editing. This is somewhat in agreement with studies showing selective ADAR1 and ADAR2 editing activities at five different editing sites within the serotonin receptor, where ADAR1 and ADAR2 can compensate for each other at some editing sites of the receptor gene, but not others [30].

Known ALS disease pathways are affected by differential RNA editing

To assess the impact of these widespread editing aberrations, we performed pathway analysis using Ingenuity Pathway Analysis (IPA) on genes that exhibited at least one RNA A to I editing aberration that occurred in all tissue types. In C9orf72 ALS/FTD spinal cord, we found enrichment of RNA editing aberrations in the Oleate Biosynthesis, EIF2 signaling, Mitochondrial L-carnitine shuttle, and the role of PKR in Interferon Induction and Antiviral Response (Fig. 5a). C9orf72 ALS/FTD motor cortex exhibited enrichment of RNA editing aberrations in transcripts related to ALS, Glutamate Receptor Signaling, and EIF2 signaling (Fig. 5b). The frontal cortex of C9orf72 ALS/FTD patients displayed enrichment in transcripts related to ALS, CREB signaling in neurons and calcium signaling (Fig. 5c). C9orf72 ALS/FTD postmortem cerebellum was enriched for EIF2 signaling, transcripts related to ALS, and Huntington's disease signaling (Fig. 5d). Of the 1458 genes that exhibit altered RNA A to I editing in C9orf72 ALS/FTD, 227 of these genes are aberrantly edited in all tissue, while 752 genes exhibit RNA editing alterations in a single tissue (Fig. 6a, Online Resource 15), indicating that each tissue type has a unique set of RNA editing aberrations which may produce different cellular responses (Fig. 6a). Gene Ontology Analysis of all genes exhibiting RNA editing aberrations revealed that transcripts related to ALS and the EIF2 signaling pathway are the most significantly mis-regulated pathways in C9orf72 ALS/FTD (Fig. 6b). Out of the 154 RNA A to I editing sites that are dysregulated in the EIF2 pathway of C9orf72 ALS/FTD patients, 16 are involved in the PI3K/AKT pathway, 35 are found in PKR or EIF2AK2, 6 in eIF2γ, 97 are found in both the 40S and the 60S ribosomal subunits (Fig. 6c). Finally, we did observe small, yet significant alterations in GluA2 Q/R editing in C9orf72 ALS/FTD spinal cord and motor cortex but not frontal cortex, cerebellum (spinal cord: 5% hyper-editing, $p = 0.02$; motor cortex: 3.47% hypo-editing, $p = 2.9e{-}10$, Online Resource 16).

Cytoplasmic ADAR2 leads to abnormal A to I editing

To assess if aberrant cytoplasmic ADAR2 is a contributing factor to alteration in A to I editing we utilized a lentiviral overexpression system to introduce a ΔNLS-ADAR2 construct in which we removed the nuclear localization sequence to force the enzyme to be present in the cytoplasm (Fig. 7a). We overexpressed these constructs in human embryonic kidney 293 cells (HEK293), a cell line that has relatively low levels of endogenous ADAR2 (Fig. 7b). ΔNLS-ADAR2 is found in the cytoplasm 48 h after transduction (Fig. 7c–e) and full length ADAR2 is properly trafficked to the nucleus under similar overexpression

a

C9orf72 ALS /FTD Spinal Cord Gene Ontology Pathways	-log(p-value)
Oleate Biosynthesis II	3.15
EIF2 Signaling	3.11
γ-linolenate Biosynthesis II	2.67
Mitochondrial L-carnitine Shuttle Pathway	2.67
Role of PKR in Interferon Induction and Antiviral Response	2.63
Stearate Biosynthesis I	2.47
IL-8 Signaling	2.41
Regulation of eIF4 and p70S6K Signaling	2.41
Fatty Acid β-oxidation I	2.4
Amyotrophic Lateral Sclerosis Signaling	2.32
Protein Ubiquitination Pathway	2.31
UDP-N-acetyl-D-galactosamine Biosynthesis II	2.29
Methylmalonyl Pathway	2.19
Superpathway of D-myo-inositol (1,4,5)-trisphosphate Metabolism	2.17
Fatty Acid Activation	2.07

b

C9orf72 ALS /FTD Motor Cortex Gene Ontology Pathways	-log(p-value)
Amyotrophic Lateral Sclerosis Signaling	3.78
Glutamate Receptor Signaling	3.67
β-alanine Degradation I	3.34
EIF2 Signaling	3.33
Valine Degradation I	3.29
TR/RXR Activation	2.84
Ephrin A Signaling	2.67
Branched-chain α-keto acid Dehydrogenase Complex	2.57
CCR3 Signaling in Eosinophils	2.54
CREB Signaling in Neurons	2.53
Regulation of eIF4 and p70S6K Signaling	2.51
Aldosterone Signaling in Epithelial Cells	2.34
Insulin Receptor Signaling	2.34
PDGF Signaling	2.28
mTOR Signaling	2.25

c

C9orf72 ALS /FTD Frontal Cortex Gene Ontology Pathways	-log(p-value)
Amyotrophic Lateral Sclerosis Signaling	5.36
CREB Signaling in Neurons	4.71
Oleate Biosynthesis II	4.7
Glutamate Receptor Signaling	3.68
β-alanine Degradation I	3.09
Calcium Signaling	3.04
G Beta Gamma Signaling	2.65
Huntington's Disease Signaling	2.58
Endocannabinoid Cancer Inhibition Pathway	2.23
GABA Receptor Signaling	2.23
Neuropathic Pain Signaling In Dorsal Horn Neurons	2.18
Cardiac β-adrenergic Signaling	2.15
TR/RXR Activation	2.1
Thrombin Signaling	2.09
Regulation of eIF4 and p70S6K Signaling	2.09

d

C9orf72 ALS /FTD Cerebellum Gene Ontology Pathways	-log(p-value)
mTOR Signaling	7.09
Amyotrophic Lateral Sclerosis Signaling	5.99
EIF2 Signaling	5.78
Huntington's Disease Signaling	4.61
CCR3 Signaling in Eosinophils	4.34
Molecular Mechanisms of Cancer	4.13
Gαq Signaling	3.6
Regulation of eIF4 and p70S6K Signaling	3.52
Docosahexaenoic Acid (DHA) Signaling	3.4
CXCR4 Signaling	3.35
Renal Cell Carcinoma Signaling	3.34
CREB Signaling in Neurons	3.31
FGF Signaling	3.27
PEDF Signaling	3.17
VEGF Family Ligand-Receptor Interactions	3.14

Fig. 5 Gene ontology analysis of all significantly mis-edited genes. Top 15 most significant canonical pathways (ingenuity pathway analysis) for genes that contain significant ($p < 0.05$, Fisher's exact test) RNA editing aberrations in C9orf72 ALS/FTD **a** spinal cord, **b** motor cortex, **c** frontal cortex, **d** cerebellum

conditions (Fig. 7f–h). We performed whole transcriptome RNA sequencing and RNA A to I editing analysis on cells expressing ΔNLS-ADAR2 and full length ADAR2. Cells with cytoplasmic ΔNLS-ADAR2 show robust alteration in RNA editing ratios compared to cells expressing full length ADAR2 (Fig. 7l). ΔNLS-ADAR2 cells display a hyper- and hypo-editing (Fig. 7l, m) phenotype, similar to C9orf72 ALS/FTD. Additionally, similar to what we found in C9orf72 ALS/FTD patient tissue, ΔNLS-ADAR2 over-expressing cells display alterations in RNA editing of PKR, the eukaryotic translation initiation factor 2 subunit alpha (eiF2α) and gamma (eiF2γ) as well as several ribosomal subunit proteins suggesting a dysregulation of protein translation in the presence of cytoplasmic ADAR2. Interestingly, direct comparison of aberrantly edited transcripts from all tissue and cellular models of ADAR2 mislocalization analyzed for RNA editing revealed editing changes in genes of the eiF2 pathway (Online Resources 17 and 18). This suggests the eiF2 pathways′ role in ribosomal function and global protein translation is possibly regulated by ADAR2 and its dysregulation might contribute to cellular dysfunction in C9orf72 ALS/FTD.

Discussion

The pathogenic disease mechanisms resulting from the hexanucleotide repeat expansion in the gene *C9orf72* are poorly understood. Here, we demonstrated the nucleocytoplasmic mislocalization of the RNA editing protein ADAR2 and a dysregulation of total A to I RNA editing in C9orf72 ALS/FTD. Unlike sporadic ALS, which displays ADAR2 downregulation, in C9orf72 mediated ALS/FTD, the RNA editing protein ADAR2 is significantly mislocalized in human tissue, human induced pluripotent stem cells, and AAV9$(G_4C_2)_{149}$ over-expressing WT mice. Dysfunction of ADAR2 in sporadic ALS has been previously suggested to be responsible for GluA2 Q/R editing deficits [32]. These RNA editing deficits result in calcium permeable AMPA receptors hypothesized to contribute to calcium induced excitotoxicity [1, 32]. GluA2 is a crucial gatekeeper for the AMPA receptor that protects against calcium permeability solely due to its ability to undergo A to I RNA editing allowing for a glutamine to arginine substitution on the ion channel of the GluA2 subunit [42]. Calcium permeable AMPA receptors have been implicated in several other neurodegenerative disorders including Alzheimer's disease and Parkinson's disease [42]. Utilizing RNA sequencing-based approaches, we detected small, yet significant RNA editing changes at the GluA2 Q/R site in C9orf72 ALS/FTD in whole tissue lysate from postmortem patient spinal cord (hyper-edited) and motor cortex (hypo-edited), but not in frontal cortex or cerebellum (Online Resource 16). The latter is consistent with a previous study using a restriction enzyme-based assay to detect GluA2 Q/R A to I editing changes in C9orf72 hiPSC-MNs [55]. The hyper-editing of

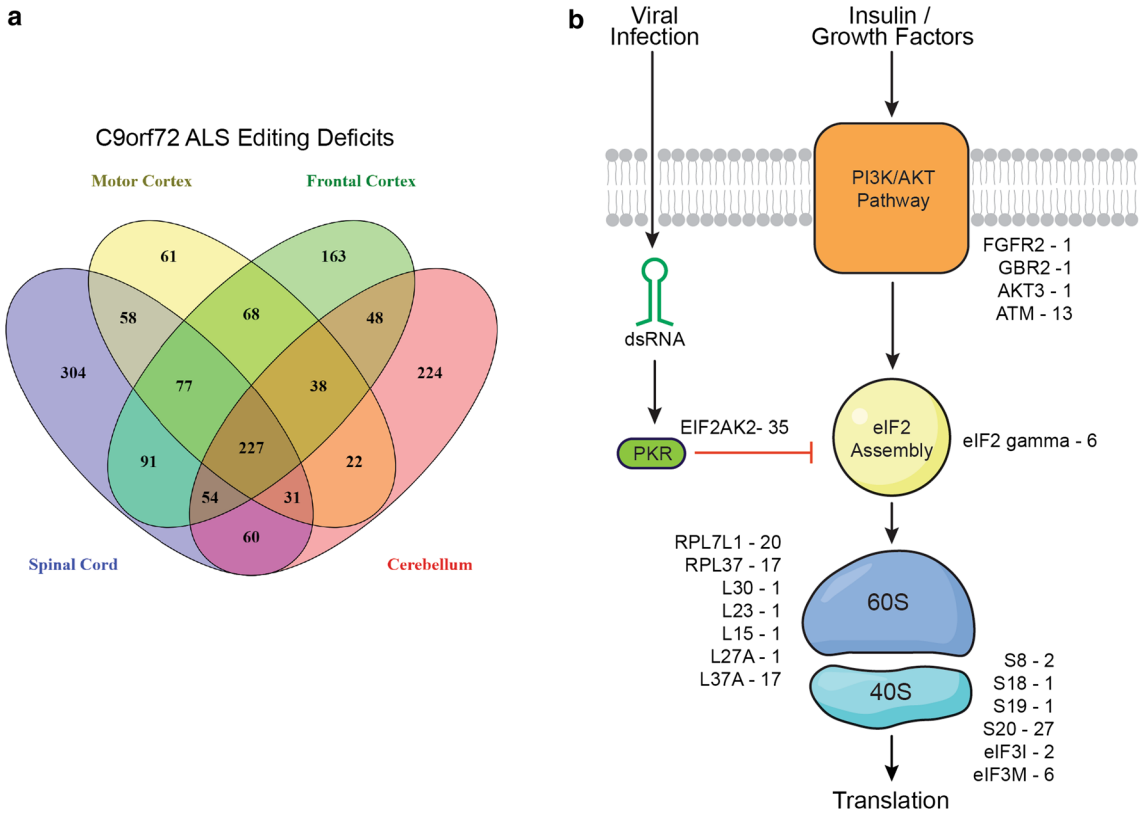

Fig. 6 Common and unique RNA editing aberrations in C9orf72 ALS/FTD. **a** Overlap of RNA A to I editing aberrations in cerebellum, frontal cortex, motor cortex and spinal cord from C9orf72 ALS/FTD tissue. **b** Annotation of the RNA editing aberrations that fall within the EIF2 signaling pathway

GluA2 Q/R in spinal cord tissue of C9orf72 ALS patients is in disagreement with prior studies in sALS patient spinal cord tissue showing hypo-editing at the GluA 2 Q/R site [39]. These studies employed laser capture microscopy (LCM) techniques to isolate spinal cord motor neurons for editing analysis [60], which could explain the differences shown in the present study using whole spinal cord tissue homogenates for RNA sequencing analysis.

The utilization of RNA sequencing technology to observe RNA editing events has allowed for a more robust characterization of altered RNA editing in disease [12, 43, 56, 57, 61]. Here, we provide evidence that global A to I editing is disturbed in C9orf72 ALS/FTD spinal cord, motor cortex, frontal cortex, and cerebellum. RNA editing in C9orf72 hiPSC-MNs is changed similarly to human tissue (Online Resources 2, 7, 10). Interestingly, the RNA editing analyses revealed both, hyper- and hypo-editing in C9orf72 tissue samples, which is in accordance with a recent RNA editing analysis from brain tissue of individuals with autism [64]. In the present study, ADAR2 gene knockdown via siRNA technology leads to similar RNA hyper- and hypo-editing changes, while additional of ADAR1 results in mostly RNA A to I hypo-editing (Online Resource 14) These data suggest that ADAR1 might be compensating at least at some select editing sites for the loss of function of ADAR2 in C9orf72 disease, in some instances even above baseline editing levels. This is somewhat in agreement with studies showing selective ADAR1 and ADAR2 editing activities at the serotonin receptor gene, which can compensate for each other at some editing site of the receptor gene, but not others [30].

RNA editing discrepancies in C9orf72 ALS/FTD show distinct, tissue-specific, aberrations. While it is not clear what impact these editing aberrations have on cellular function, these RNA editing events may be initial clues describing selective vulnerability in ALS. However, future studies need to determine the specific mechanisms of RNA editing toxicity in ALS. Pathway analysis of total RNA discrepancies revealed the eIF2 pathway to be the most disrupted by RNA editing aberrations in C9orf72 ALS/FTD. Editing aberrations within this pathway are observed in all models of abnormal RNA editing (Online Resources 17 and 18). The eukaryotic initiation factor 2 pathway is a crucial element required for the initiation of neuron-specific translation and assembly of the initiation ternary complex containing eIF2-Met-tRNAi-GTP [15, 36]. Our analysis revealed significant RNA editing aberrations in this pathway, indicating

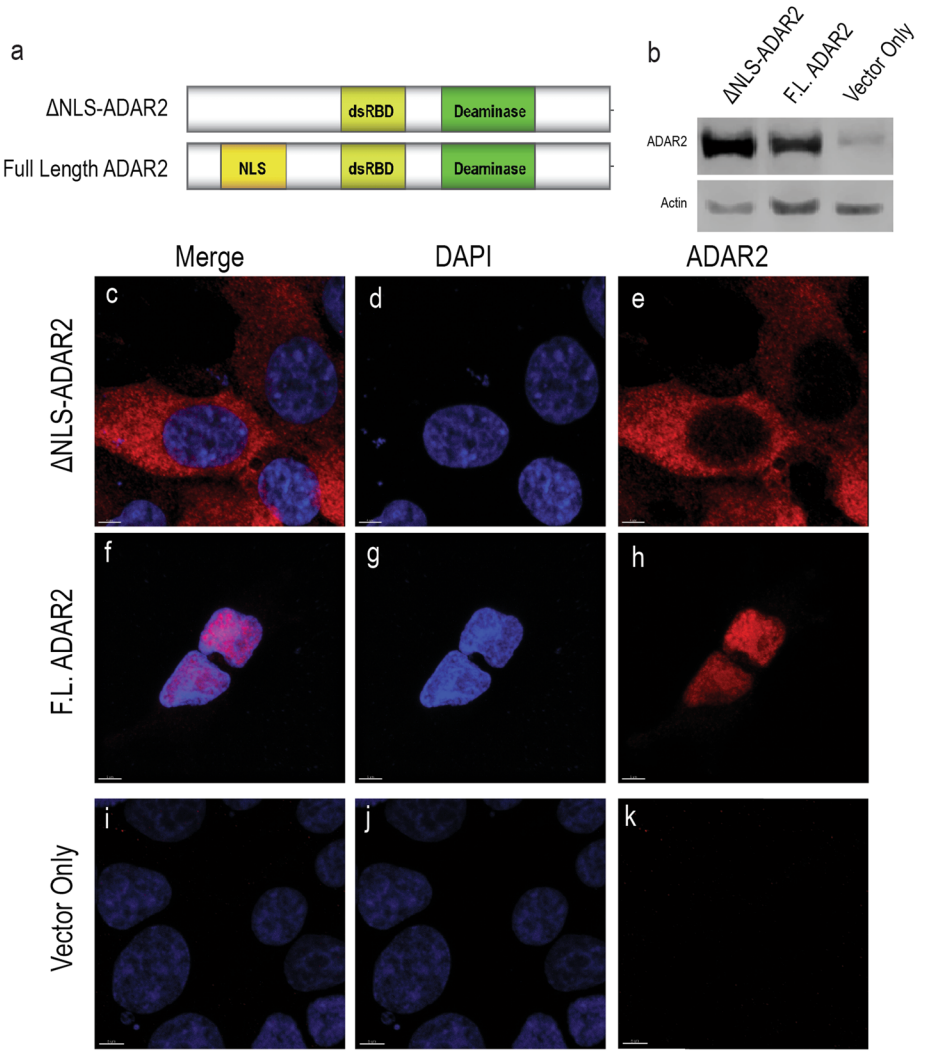

l

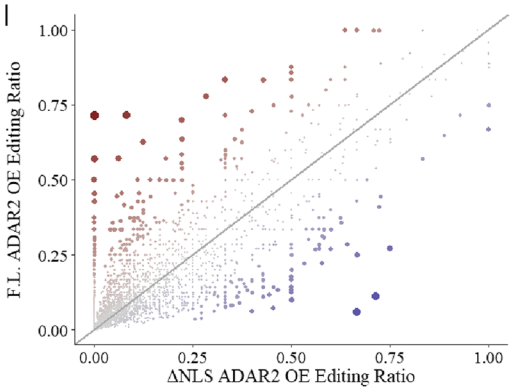

m

Gene	Change in Editing (%)
RILPL1	-71.43
HELLS	-63.1
KNOP1	-57.1
TGOLN2	-50.89
TIPIN	-50
DUSP18	40
ACOX1	41.67
SMYD4	47.79
XPNPEP3	60.32
DOC2A	60.78

n

Gene	Name	Editing Site	Change in A to I Editing
EIF2AK2	Protein Kinase R	chr2_37327702	-50.00
EIF2S1	Eukaryotic Translation Initiation Factor 2 Subunit Alpha	chr14_67852067	-10.00
EIF2S3	Eukaryotic Translation Initiation Factor 2 Subunit Gamma	chrX_24094068	-10.00
RPL7L1	Ribosomal Protein L7 Like 1	chr6_42856039	-30.00
RPL13	Large Ribosomal Subunit Protein EL13	chr16_89630036	-12.50
RPL23	Ribosomal Protein L23	chr17_37006223	-33.33
RPL23A	Ribosomal Protein L23a	chr17_27049326	20.83
RPL30	Ribosomal Protein L30	chr8_99055492	20.83

Fig. 7 Cytoplasmic ADAR2 leads to altered RNA editing. **a** Schematics of both ΔNLS-ADAR2 and full-length lentiviral constructs. **b** Western blot showing successful transduction of both ΔNLS-ADAR2 and full length ADAR2 in HEK293 cells. **c**–**e** ΔNLS-ADAR2 is localized to the cytoplasm. **f**–**h** Full length ADAR2 is trafficked to the nucleus. **i**–**k** Cells treated with an empty vector control. **l** Whole transcriptome RNA sequencing reveals that there are alterations in the editing ratios between cells expressing a nuclear ADAR2 and a cytoplasmic ADAR2. **m** Most substantially misedited genes that are decreased (red) and increased (blue) in cells expressing ΔNLS-ADAR2. **n** EIF2AK2, EIF2S1, EIF2S3, and Ribosomal subunits are differentially edited in cells expressing ADAR2 in the cytoplasm

possible dysfunction. The eIF2α kinase, Protein Kinase R (PKR) is one of the transcripts showing large RNA editing dysfunction. PKR is an interferon-inducible, double-stranded RNA-activated protein kinase, and activation of PKR leads to the phosphorylation of eIF2α at residue S51 and the inhibition of the GDP and GTP exchange leading to an inhibition of global translation and cellular susceptibility to non-AUG based translation [51]. ADAR1 acts as a suppressor of PKR, suggesting that not only ADAR2 A to I editing targets, but, additionally, ADAR1 targets, might be dysregulated in C9orf72 ALS/FTD. eIF2α phosphorylation is associated with neurodegenerative disease, including Alzheimer's disease, Parkinson's disease, Huntington's disease, and ALS/FTD [7, 20, 31]. Expression of the *C9orf72* repeat expansion has recently been shown to activate the integrated stress response by phosphorylation of eIF2α [14]. Although the RNA alterations observed in the PKR transcript are the most well understood, we also identified several other RNA editing aberrations involved in the same pathway, including aberrations involved in the eIF2 subunits themselves and aberrations found in the ribosomal subunits, indicating the potential for further dysregulation of this pathway. Further studies are necessary to understand the function of the pathogenic, or even the beneficial, impact of these RNA editing aberrations.

Acknowledgements We would like to thank the Sattler Laboratory for suggestions and comments towards the manuscript. We would also like to thank all ALS patients and families that have contributed to this research via postmortem brain tissue donations. Specifically, we would like to thank Doug Clough for assistance with data analysis and insightful discussions. We further thank the Target ALS Human Postmortem Tissue Core, New York Genome Center for Genomics of Neurodegenerative Disease, Amyotrophic Lateral Sclerosis Association and TOW Foundation for providing access to their postmortem patient tissue samples collection. We thank both the Target ALS Consortium and the New York Genome Center for access to their RNA sequencing database. In particular, we would like to thank Drs. Lyle Ostrow, Hemali Phatnani and Robert Bowser. We would also like to thank Drs. Sylvia Perez and Elliott Mufson for generously providing us with AD patient postmortem tissue samples. Further thanks go to Dr. Stella Dracheva for helpful discussions throughout this project. This work was support by the National Institute of Neurological Disorders and Stroke, NIH RO1NS085207 (RS); the Muscular Dystrophy Association (RS); the ALS Association (RS); the Robert Packard Center for ALS Research (RS); and the Barrow Neurological Foundation (RS). Part of this work was also made possible by NIH Grant R01NS097850 (JKI), US Department of Defense Grant W81XWH-15-1-0187 (JI), and grants from the Donald E. and Delia B. Baxter Foundation (JKI), the Alzheimer's Drug Discovery Foundation (JKI) and the Association for Frontotemporal Degeneration (JKI), the Harrington Discovery Institute (JKI), the Tau Consortium (JKI), the Pape Adams Foundation (JKI), the Frick Foundation for ALS Research (JKI), the Muscular Dystrophy Association (JKI), the New York Stem Cell Foundation (JKI), the USC Keck School of Medicine Regenerative Medicine Initiative (JKI), the USC Broad Innovation Award (JKI), and the Southern California Clinical and Translational Science Institute to JKI. JKI is a New York Stem Cell Foundation-Robertson Investigator and a Richard N. Merkin Scholar. We would additionally like to thank the National Institutes of Health/National Institute of Neurological Disorders and Stroke [R35NS097273 (L.P.); P01NS084974 (L.P.); P01NS099114 (L.P.); R01NS088689 (L.P.)]; the Mayo Clinic Foundation (L.P.); the Amyotrophic Lateral Sclerosis Association (L.P.), the Robert Packard Center for ALS Research at Johns Hopkins (L.P.), the Target ALS Foundation (L.P.), and the James Hunter Family ALS Initiative (JR).

References

1. Akamatsu M, Yamashita T, Hirose N, Teramoto S, Kwak S (2016) The AMPA receptor antagonist perampanel robustly rescues amyotrophic lateral sclerosis (ALS) pathology in sporadic ALS model mice. Sci Rep 6:28649. https://doi.org/10.1038/srep28649
2. Almeida S, Gascon E, Tran H, Chou HJ, Gendron TF, Degroot S et al (2013) Modeling key pathological features of frontotemporal dementia with C9ORF72 repeat expansion in iPSC-derived human neurons. Acta Neuropathol 126:385–399. https://doi.org/10.1007/s00401-013-1149-y
3. Ash Peter EA, Bieniek Kevin F, Gendron Tania F, Caulfield T, Lin W-L, DeJesus-Hernandez M et al (2013) Unconventional translation of C9ORF72 GGGGCC expansion generates insoluble polypeptides specific to c9FTD/ALS. Neuron 77:639–646. https://doi.org/10.1016/j.neuron.2013.02.004
4. Atanasio A, Decman V, White D, Ramos M, Ikiz B, Lee HC et al (2016) C9orf72 ablation causes immune dysregulation characterized by leukocyte expansion, autoantibody production, and glomerulonephropathy in mice. Sci Rep 6:23204. https://doi.org/10.1038/srep23204
5. Bass BL, Weintraub H (1987) A developmentally regulated activity that unwinds RNA duplexes. Cell 48:607–613. https://doi.org/10.1016/0092-8674(87)90239-X
6. Behm M, Wahlstedt H, Widmark A, Eriksson M, Ohman M (2017) Accumulation of nuclear ADAR2 regulates adenosine-to-inosine RNA editing during neuronal development. J Cell Sci 130:745–753. https://doi.org/10.1242/jcs.200055
7. Bell MC, Meier SE, Ingram AL, Abisambra JF (2016) PERK-opathies: an endoplasmic reticulum stress mechanism underlying neurodegeneration. Curr Alzheimer Res 13:150–163
8. Belzil VV, Bauer PO, Prudencio M, Gendron TF, Stetler CT, Yan IK et al (2013) Reduced C9orf72 gene expression in c9FTD/ALS is caused by histone trimethylation, an epigenetic event detectable in blood. Acta Neuropathol 126:895–905. https://doi.org/10.1007/s00401-013-1199-1
9. Boeynaems S, Bogaert E, Michiels E, Gijselinck I, Sieben A, Jovičić A et al (2016) Drosophila screen connects nuclear transport genes to DPR pathology in c9ALS/FTD. Sci Rep 6: 20877. https://doi.org/10.1038/srep20877. http://www.nature.com/articles/srep20877—supplementary-information
10. Boeynaems S, Bogaert E, Van Damme P, Van Den Bosch L (2016) Inside out: the role of nucleocytoplasmic transport in ALS and FTLD. Acta Neuropathol 132:159–173. https://doi.org/10.1007/s00401-016-1586-5
11. Burberry A, Suzuki N, Wang J-Y, Moccia R, Mordes DA, Stewart MH et al (2016) Loss-of-function mutations in the *C9ORF72* mouse ortholog cause fatal autoimmune disease. Sci Transl Med 8:347ra393
12. Cesarini V, Silvestris DA, Tassinari V, Tomaselli S, Alon S, Eisenberg E et al (2017) ADAR2/miR-589-3p axis controls glioblastoma cell migration/invasion. Nucleic Acids Res. https://doi.org/10.1093/nar/gkx1257
13. Chen CX, Cho DS, Wang Q, Lai F, Carter KC, Nishikura K (2000) A third member of the RNA-specific adenosine deaminase gene family, ADAR3, contains both single- and double-stranded RNA binding domains. RNA 6:755–767

14. Cheng W, Wang S, Mestre AA, Fu C, Makarem A, Xian F et al (2018) C9ORF72 GGGGCC repeat-associated non-AUG translation is upregulated by stress through eIF2α phosphorylation. Nat Commun 9:51. https://doi.org/10.1038/s41467-017-02495-z
15. Chesnokova E, Bal N, Kolosov P (2017) Kinases of eIF2a switch translation of mRNA subset during neuronal plasticity. Int J Mol Sci. https://doi.org/10.3390/ijms18102213
16. Chew J, Cook C, Gendron TF, Jansen-West K, Del Rosso G, Daughrity LM et al (2019) Aberrant deposition of stress granule-resident proteins linked to C9orf72-associated TDP-43 proteinopathy. Mol Neurodegener 14:9. https://doi.org/10.1186/s13024-019-0310-z
17. Ciura S, Lattante S, Le Ber I, Latouche M, Tostivint H, Brice A et al (2013) Loss of function of C9orf72 causes motor deficits in a zebrafish model of amyotrophic lateral sclerosis. Ann Neurol 74:180–187. https://doi.org/10.1002/ana.23946
18. Connell MA, Krause S, Higuchi M, Hsuan JJ, Totty NF, Jenny A et al (1995) Cloning of cDNAs encoding mammalian double-stranded RNA-specific adenosine deaminase. Mol Cell Biol 15:1389
19. DeJesus-Hernandez M, Mackenzie Ian R, Boeve Bradley F, Boxer Adam L, Baker M, Rutherford Nicola J et al (2011) Expanded GGGGCC hexanucleotide repeat in noncoding region of C9ORF72 causes chromosome 9p-linked FTD and ALS. Neuron 72:245–256. https://doi.org/10.1016/j.neuron.2011.09.011
20. Devi L, Ohno M (2014) PERK mediates eIF2α phosphorylation responsible for BACE1 elevation, CREB dysfunction and neurodegeneration in a mouse model of Alzheimer's disease. Neurobiol Aging 35:2272–2281. https://doi.org/10.1016/j.neurobiolaging.2014.04.031
21. Donnelly CJ, Zhang PW, Pham JT, Heusler AR, Mistry NA, Vidensky S et al (2013) RNA toxicity from the ALS/FTD C9ORF72 expansion is mitigated by antisense intervention. Neuron 80:415–428. https://doi.org/10.1016/j.neuron.2013.10.015
22. Eftekharzadeh B, Daigle JG, Kapinos LE, Coyne A, Schiantarelli J, Carlomagno Y et al (2018) Tau protein disrupts nucleocytoplasmic transport in Alzheimer's disease. Neuron 99(925–940):e927. https://doi.org/10.1016/j.neuron.2018.07.039
23. Franzén O, Ermel R, Sukhavasi K, Jain R, Jain A, Betsholtz C et al (2018) Global analysis of A-to-I RNA editing reveals association with common disease variants. PeerJ 6:e4466. https://doi.org/10.7717/peerj.4466
24. Freibaum BD, Lu Y, Lopez-Gonzalez R, Kim NC, Almeida S, Lee K-H et al (2015) GGGGCC repeat expansion in C9orf72 compromises nucleocytoplasmic transport. Nature 525:129. https://doi.org/10.1038/nature14974. http://www.nature.com/articles/nature14974—supplementary-information
25. Gasset-Rosa F, Chillon-Marinas C, Goginashvili A, Atwal RS, Artates JW, Tabet R et al (2017) Polyglutamine-expanded huntingtin exacerbates age-related disruption of nuclear integrity and nucleocytoplasmic transport. Neuron 94(48–57):e44. https://doi.org/10.1016/j.neuron.2017.03.027
26. Gendron TF, van Blitterswijk M, Bieniek KF, Daughrity LM, Jiang J, Rush BK et al (2015) Cerebellar c9RAN proteins associate with clinical and neuropathological characteristics of C9ORF72 repeat expansion carriers. Acta Neuropathol 130:559–573. https://doi.org/10.1007/s00401-015-1474-4
27. Gijselinck I, Van Langenhove T, van der Zee J, Sleegers K, Philtjens S, Kleinberger G et al (2012) A C9orf72 promoter repeat expansion in a Flanders-Belgian cohort with disorders of the frontotemporal lobar degeneration-amyotrophic lateral sclerosis spectrum: a gene identification study. Lancet Neurol 11:54–65. https://doi.org/10.1016/S1474-4422(11)70261-7
28. Grima JC, Daigle JG, Arbez N, Cunningham KC, Zhang K, Ochaba J et al (2017) Mutant huntingtin disrupts the nuclear pore complex. Neuron 94(93–107):e106. https://doi.org/10.1016/j.neuron.2017.03.023
29. Haeusler AR, Donnelly CJ, Rothstein JD (2016) The expanding biology of the C9orf72 nucleotide repeat expansion in neurodegenerative disease. Nat Rev Neurosci 17:383. https://doi.org/10.1038/nrn.2016.38. http://www.nature.com/articles/nrn.2016.38—supplementary-information
30. Hartner JC, Schmittwolf C, Kispert A, Muller AM, Higuchi M, Seeburg PH (2004) Liver disintegration in the mouse embryo caused by deficiency in the RNA-editing enzyme ADAR1. J Biol Chem 279:4894–4902. https://doi.org/10.1074/jbc.M311347200
31. Hetz C, Mollereau B (2014) Disturbance of endoplasmic reticulum proteostasis in neurodegenerative diseases. Nat Rev Neurosci 15:233. https://doi.org/10.1038/nrn3689
32. Hideyama T, Yamashita T, Aizawa H, Tsuji S, Kakita A, Takahashi H et al (2012) Profound downregulation of the RNA editing enzyme ADAR2 in ALS spinal motor neurons. Neurobiol Dis 45:1121–1128. https://doi.org/10.1016/j.nbd.2011.12.033
33. Hideyama T, Yamashita T, Suzuki T, Tsuji S, Higuchi M, Seeburg PH et al (2010) Induced loss of ADAR2 engenders slow death of motor neurons from Q/R site-unedited GluR2. J Neurosci 30:11917–11925. https://doi.org/10.1523/JNEUROSCI.2021-10.2010
34. Higuchi M, Maas S, Single FN, Hartner J, Rozov A, Burnashev N et al (2000) Point mutation in an AMPA receptor gene rescues lethality in mice deficient in the RNA-editing enzyme ADAR2. Nature 406:78–81. https://doi.org/10.1038/35017558
35. Hwang T, Park CK, Leung AK, Gao Y, Hyde TM, Kleinman JE et al (2016) Dynamic regulation of RNA editing in human brain development and disease. Nat Neurosci 19:1093–1099. https://doi.org/10.1038/nn.4337
36. Jackson RJ, Hellen CUT, Pestova TV (2010) The mechanism of eukaryotic translation initiation and principles of its regulation. Nat Rev Mol Cell Biol 11:113. https://doi.org/10.1038/nrm2838. http://www.nature.com/articles/nrm2838—supplementary-information
37. Jovičić A, Mertens J, Boeynaems S, Bogaert E, Chai N, Yamada SB et al (2015) Modifiers of C9orf72 dipeptide repeat toxicity connect nucleocytoplasmic transport defects to FTD/ALS. Nat Neurosci 18:1226. https://doi.org/10.1038/nn.4085. http://www.nature.com/articles/nn.4085—supplementary-information
38. Kim U, Wang Y, Sanford T, Zeng Y, Nishikura K (1994) Molecular cloning of cDNA for double-stranded RNA adenosine deaminase, a candidate enzyme for nuclear RNA editing. Proc Natl Acad Sci 91:11457
39. Kwak S, Kawahara Y (2005) Deficient RNA editing of GluR2 and neuronal death in amyotropic lateral sclerosis. J Mol Med 83:110–120. https://doi.org/10.1007/s00109-004-0599-z
40. Lagier-Tourenne C, Baughn M, Rigo F, Sun S, Liu P, Li H-R et al (2013) Targeted degradation of sense and antisense *C9orf72* RNA foci as therapy for ALS and frontotemporal degeneration. Proc Natl Acad Sci 110:E4530
41. Lee Y-B, Chen H-J, Peres João N, Gomez-Deza J, Attig J, Štalekar M et al (2013) Hexanucleotide repeats in ALS/FTD form length-dependent RNA foci, sequester RNA binding proteins, and are neurotoxic. Cell Rep 5:1178–1186. https://doi.org/10.1016/j.celrep.2013.10.049
42. Lorenzini I, Moore S, Sattler R (2018) RNA editing deficiency in neurodegeneration. Adv Neurobiol 20:63–83. https://doi.org/10.1007/978-3-319-89689-2_3
43. Maemura K, Watanabe K, Ando T, Hiyama N, Sakatani T, Amano Y et al (2018) Altered editing level of microRNAs is a potential biomarker in lung adenocarcinoma. Cancer Sci. https://doi.org/10.1111/cas.13742
44. May S, Hornburg D, Schludi MH, Arzberger T, Rentzsch K, Schwenk BM et al (2014) C9orf72 FTLD/ALS-associated

Gly-Ala dipeptide repeat proteins cause neuronal toxicity and Unc119 sequestration. Acta Neuropathol 128:485–503. https://doi.org/10.1007/s00401-014-1329-4
45. Melcher T, Maas S, Higuchi M, Keller W, Seeburg PH (1995) Editing of alpha-amino-3-hydroxy-5-methylisoxazole-4-propionic acid receptor GluR-B pre-mRNA in vitro reveals site-selective adenosine to inosine conversion. J Biol Chem 270:8566–8570
46. Mizielinska S, Grönke S, Niccoli T, Ridler CE, Clayton EL, Devoy A et al (2014) *C9orf72* repeat expansions cause neurodegeneration in *Drosophila* through arginine-rich proteins. Science 345:1192
47. Mohan A, Goodwin M, Swanson MS (2014) RNA–protein interactions in unstable microsatellite diseases. Brain Res 1584:3–14. https://doi.org/10.1016/j.brainres.2014.03.039
48. Mori K, Weng S-M, Arzberger T, May S, Rentzsch K, Kremmer E et al (2013) The *C9orf72* GGGGCC repeat is translated into aggregating dipeptide-repeat proteins in FTLD/ALS. Science 339:1335
49. Orecchini E, Frassinelli L, Galardi S, Ciafre SA, Michienzi A (2018) Post-transcriptional regulation of LINE-1 retrotransposition by AID/APOBEC and ADAR deaminases. Chromosome Res Int J Mol Supramol Evol Asp Chromosome Biol 26:45–59. https://doi.org/10.1007/s10577-018-9572-5
50. Paonessa F, Evans LD, Solanki R, Larrieu D, Wray S, Hardy J et al (2019) Microtubules deform the nuclear membrane and disrupt nucleocytoplasmic transport in tau-mediated frontotemporal dementia. Cell Rep 26(582–593):e585. https://doi.org/10.1016/j.celrep.2018.12.085
51. Pfaller CK, Li Z, George CX, Samuel CE (2011) Protein kinase PKR and RNA adenosine deaminase ADAR1: new roles for old players as modulators of the interferon response. Curr Opin Immunol 23:573–582. https://doi.org/10.1016/j.coi.2011.08.009
52. Reed SE, Staley EM, Mayginnes JP, Pintel DJ, Tullis GE (2006) Transfection of mammalian cells using linear polyethylenimine is a simple and effective means of producing recombinant adeno-associated virus vectors. J Virol Methods 138:85–98. https://doi.org/10.1016/j.jviromet.2006.07.024
53. Renton Alan E, Majounie E, Waite A, Simón-Sánchez J, Rollinson S, Gibbs JR et al (2011) A hexanucleotide repeat expansion in C9ORF72 is the cause of chromosome 9p21-linked ALS-FTD. Neuron 72:257–268. https://doi.org/10.1016/j.neuron.2011.09.010
54. Sareen D, O'Rourke JG, Meera P, Muhammad AKMG, Grant S, Simpkinson M et al (2013) Targeting RNA foci in iPSC-derived motor neurons from ALS patients with a *C9ORF72* repeat expansion. Sci Transl Med 5:208ra149
55. Selvaraj BT, Livesey MR, Zhao C, Gregory JM, James OT, Cleary EM et al (2018) C9ORF72 repeat expansion causes vulnerability of motor neurons to Ca^{2+}-permeable AMPA receptor-mediated excitotoxicity. Nat Commun 9:347. https://doi.org/10.1038/s41467-017-02729-0
56. Sharpnack MF, Chen B, Aran D, Kosti I, Sharpnack DD, Carbone DP et al (2018) Global transcriptome analysis of RNA abundance regulation by ADAR in lung adenocarcinoma. EBioMedicine 27:167–175. https://doi.org/10.1016/j.ebiom.2017.12.005
57. Shelton PM, Duran A, Nakanishi Y, Reina-Campos M, Kasashima H, Llado V et al (2018) The secretion of miR-200s by a PKCζ/ADAR2 signaling axis promotes liver metastasis in colorectal cancer. Cell Rep 23:1178–1191. https://doi.org/10.1016/j.celrep.2018.03.118
58. Shi Y, Lin S, Staats KA, Li Y, Chang W-H, Hung S-T et al (2018) Haploinsufficiency leads to neurodegeneration in C9ORF72 ALS/FTD human induced motor neurons. Nat Med 24:313. https://doi.org/10.1038/nm.4490. http://www.nature.com/articles/nm.4490—supplementary-information
59. Sun W, Samimi H, Gamez M, Zare H, Frost B (2018) Pathogenic tau-induced piRNA depletion promotes neuronal death through transposable element dysregulation in neurodegenerative tauopathies. Nat Neurosci 21:1038–1048. https://doi.org/10.1038/s41593-018-0194-1
60. Takuma H, Kwak S, Yoshizawa T, Kanazawa I (1999) Reduction of GluR2 RNA editing, a molecular change that increases calcium influx through AMPA receptors, selective in the spinal ventral gray of patients with amyotrophic lateral sclerosis. Ann Neurol 46:806–815
61. Tan MH, Li Q, Shanmugam R, Piskol R, Kohler J, Young AN et al (2017) Dynamic landscape and regulation of RNA editing in mammals. Nature 550:249–254. https://doi.org/10.1038/nature24041
62. Therrien M, Rouleau GA, Dion PA, Parker JA (2013) Deletion of C9ORF72 results in motor neuron degeneration and stress sensitivity in *C. elegans*. PLOS ONE 8:e83450. https://doi.org/10.1371/journal.pone.0083450
63. Tran H, Almeida S, Moore J, Gendron Tania F, Chalasani U, Lu Y et al (2015) Differential toxicity of nuclear RNA foci versus dipeptide repeat proteins in a *Drosophila* model of C9ORF72 FTD/ALS. Neuron 87:1207–1214. https://doi.org/10.1016/j.neuron.2015.09.015
64. Tran SS, Jun HI, Bahn JH, Azghadi A, Ramaswami G, Van Nostrand EL et al (2019) Widespread RNA editing dysregulation in brains from autistic individuals. Nat Neurosci 22:25–36. https://doi.org/10.1038/s41593-018-0287-x
65. Vucic S, Rothstein JD, Kiernan MC (2014) Advances in treating amyotrophic lateral sclerosis: insights from pathophysiological studies. Trends Neurosci 37:433–442. https://doi.org/10.1016/j.tins.2014.05.006
66. Waite AJ, Bäumer D, East S, Neal J, Morris HR, Ansorge O et al (2014) Reduced C9orf72 protein levels in frontal cortex of amyotrophic lateral sclerosis and frontotemporal degeneration brain with the C9ORF72 hexanucleotide repeat expansion. Neurobiol Aging 35:1779.e5–1779.e13. https://doi.org/10.1016/j.neurobiolaging.2014.01.016
67. Wang Q, Khillan J, Gadue P, Nishikura K (2000) Requirement of the RNA editing deaminase ADAR1 gene for embryonic erythropoiesis. Science 290:1765
68. Wang Q, Miyakoda M, Yang W, Khillan J, Stachura DL, Weiss MJ et al (2004) Stress-induced apoptosis associated with null mutation of ADAR1 RNA editing deaminase gene. J Biol Chem 279:4952–4961. https://doi.org/10.1074/jbc.M310162200
69. Wen X, Tan W, Westergard T, Krishnamurthy K, Markandaiah SS, Shi Y et al (2014) Antisense proline-arginine RAN dipeptides linked to C9ORF72-ALS/FTD form toxic nuclear aggregates that initiate in vitro and in vivo neuronal death. Neuron 84:1213–1225. https://doi.org/10.1016/j.neuron.2014.12.010
70. Xiao S, MacNair L, McGoldrick P, McKeever PM, McLean JR, Zhang M et al (2015) Isoform-specific antibodies reveal distinct subcellular localizations of C9orf72 in amyotrophic lateral sclerosis. Ann Neurol 78:568–583. https://doi.org/10.1002/ana.24469
71. Yang D, Abdallah A, Li Z, Lu Y, Almeida S, Gao F-B (2015) FTD/ALS-associated poly(GR) protein impairs the Notch pathway and is recruited by poly(GA) into cytoplasmic inclusions. Acta Neuropathol 130:525–535. https://doi.org/10.1007/s00401-015-1448-6
72. Yu W, Xu H, Xue Y, An D, Li H, Chen W et al (2018) 5-HT2CR antagonist/5-HT2CR inverse agonist recovered the increased isolation-induced aggressive behavior of BALB/c mice mediated by ADAR1 (p110) expression and Htr2c RNA editing. Brain Behav 8:e00929. https://doi.org/10.1002/brb3.929
73. Zhang K, Donnelly CJ, Haeusler AR, Grima JC, Machamer JB, Steinwald P et al (2015) The C9orf72 repeat expansion disrupts nucleocytoplasmic transport. Nature 525:56. https://doi.org/10.1038/nature14973. http://www.nature.com/articles/nature14973—supplementary-information

74. Zhang Y-J, Gendron TF, Ebbert MTW, O'Raw AD, Yue M, Jansen-West K et al (2018) Poly(GR) impairs protein translation and stress granule dynamics in C9orf72-associated frontotemporal dementia and amyotrophic lateral sclerosis. Nat Med 24:1136–1142. https://doi.org/10.1038/s41591-018-0071-1
75. Zhang Y-J, Jansen-West K, Xu Y-F, Gendron TF, Bieniek KF, Lin W-L et al (2014) Aggregation-prone c9FTD/ALS poly(GA) RAN-translated proteins cause neurotoxicity by inducing ER stress. Acta Neuropathol 128:505–524. https://doi.org/10.1007/s00401-014-1336-5
76. Zu T, Liu Y, Bañez-Coronel M, Reid T, Pletnikova O, Lewis J et al (2013) RAN proteins and RNA foci from antisense transcripts in *C9ORF72* ALS and frontotemporal dementia. Proc Natl Acad Sci 110:E4968